A Boundary Fitted Nested Grid Model for Modelling Tsunami Propagation of 2004 Indonesian Tsunami along Southern Thailand

Md. Fazlul Karim, Esa Al-Islam

Abstract—This paper describes the development of a boundary fitted nested grid (BFNG) model to compute tsunami propagation of 2004 Indonesian tsunami in Southern Thailand coastal waters. We develop a numerical model employing the shallow water nested model and an orthogonal boundary fitted grid to investigate the tsunami impact on the Southern Thailand due to the Indonesian tsunami of 2004. Comparisons of water surface elevation obtained from numerical simulations and field measurements are made.

Keywords—Boundary-fitted nested grid model, finite difference method, Indonesian tsunami of 2004, Southern Thailand.

I. INTRODUCTION

A tsunami is generated due to undersea earthquake when plate boundaries deform abruptly and a large amount of the overlying water in the ocean move vertically. When earthquakes occur under the sea, the water over the deformed zone is displaced from the equilibrium position. Tsunamis are formed when the displaced water tries to regain equilibrium.

The Indonesian tsunami of 2004 started with a main shock, located ≈ 160 km west of North Sumatra, at a depth of $25 - 30$ km. Seismic models indicate that the main shock and associated rupture propagated northward from the epicenter, parallel to the trenches, at a shear wave speed of $2 - 3$ km/s for ~500 s and thus covering the ~ 1200 km length of the ruptured fault (Fig. 6) [2]. Moreover, the extent of rupture between 93–97°E and 3–11°N with the amount of maximum se abed rise is 507 cm at the west and maximum fall of 474 cm at the east was reported in [12] and this estimation is based on elastic deformation theory of Okada [15]. This event originated at Sumatra and was felt all over the rim countries of the Indian Ocean and had a severe impact on the Phuket Island in Southern Thailand. The west coast of Southern Thailand faces the Sumatra Island where there is an active seismic tsunami source. Phuket Island was lashed by high tsunami surges due to that event and thus appears to be vulnerable for high surge due to the source. Hence, attention should be given on prediction of tsunami along the coastal belt of southern Thailand.

After the historical event, considerable research has been done and many of the past studies for the event which occurred

M.F. Karim is with the Institut Teknologi Brunei, Brunei (phone: +673 7157167; e-mail: mdfazlulkk@yahoo.com, fazlul.karim@itb.edu.bn).

E. A. Islam is with the Institut Teknologi Brunei, Brunei (e-mail: esa.yunus@itb.edu.bn).

at Sumatra on December 2004 along the coastal belt of southern Thailand are based on field surveys. Notable studies were made by [14], [13], [18], Tsuji et al. [19]. A significant number of works based on numerical simulation for determining the impact for the above region have also been carried out. These include [16], [17], [12], [7]–[9]. In [17] and [7]–[9] Cartesian coordinate shallow water models were used but the rupture velocity and the rise time were neglected. In those studies, it was assumed that the initial displacement of the sea surface is equal to the sudden and permanent shift of sea bed and the sea surface enhancement is considered instantaneous. The main reason for determining the initial size of a tsunami is the relation to the amount of vertical sea bed deformation over a short period of time [4]. A global model in spherical polar coordinate shallow water model to simulate the Indonesian tsunami of 2004 event throughout the globe between 80°S and 69°N was developed by [12].

The coastal boundaries of Southern Thailand (Fig. 1) and the island boundaries of Phuket (Fig. 2) are curvilinear in nature and the model domain covers shallow water (near the beach) and the deep sea (east of Indian Ocean), and thus abrupt differences of velocities are expected near the beach. In spite of a considerable number of papers have been published for these regions [7]–[9], [17], [16] details of rupture process at source zone, bathymetry of the shore and orography of the coastal belts are still not well understood.

Many problems in oceanography and environmental sciences require the solution of shallow water equations on physical domains having curvilinear coastlines and abrupt changes of ocean depth near the shore. Finite-difference technique for the shallow water equations representing the boundary as stair step may give inaccurate results near the coastline where results are of greatest interest for various applications. This suggests the use of methods which are capable of incorporating the irregular boundary in coastal belts. At the same time, large velocity gradient is expected near the beach and islands as water depth varies abruptly near the coast. A nested numerical scheme with fine resolution is the best resort to enhance the numerical accuracy with the least grid numbers for the region of interests where the velocity changes rapidly and which is unnecessary for the away of the region [1], [3], [8].

This study employs the concept of boundary-fitted coordinates to allow for an accurate representation of coastal and island boundaries of the Phuket while retaining the

World Academy of Science, Engineering and Technology
International Journal of Geological and Environmental Engineering
Vol:9, No:8, 2015

simplicity of the finite difference method of solution process. Although a general curvilinear coordinate system covers the physical domain, all simulations to solve the governing equations of shallow water equations, as well as the computation of the boundary-fitted coordinate system, are performed in a transformed rectangular domain with equally spaced grid. Moreover, in order to increase the accuracy of simulation results from deep ocean coarse resolution, nested grids with fine resolution are employed to shallow regions near the shore where the bathymetry changes rapidly. The advantage of such a model is that this boundary-fitted technique makes the governing equations and boundary conditions simple and represents the coastal and island

boundaries accurately [5]. Moreover, nested scheme within the outer model can record the specification of lateral boundary conditions to nested grid domain(s) in a more realistic manner and thus improve the results of simulation of oceanic phenomena [10], [11]. This is particularly important for Phuket region. This study also considers a more realistic initial condition of tsunami generation by taking into account the dynamics of sea bed deformation over a short period of time. The assumption considered in previous studies [17], [8], [9] that the initial displacement of the sea surface is equal to sudden and permanent shift of the sea bed and the sea surface enhancement being considered instantaneous will be dropped in this study.
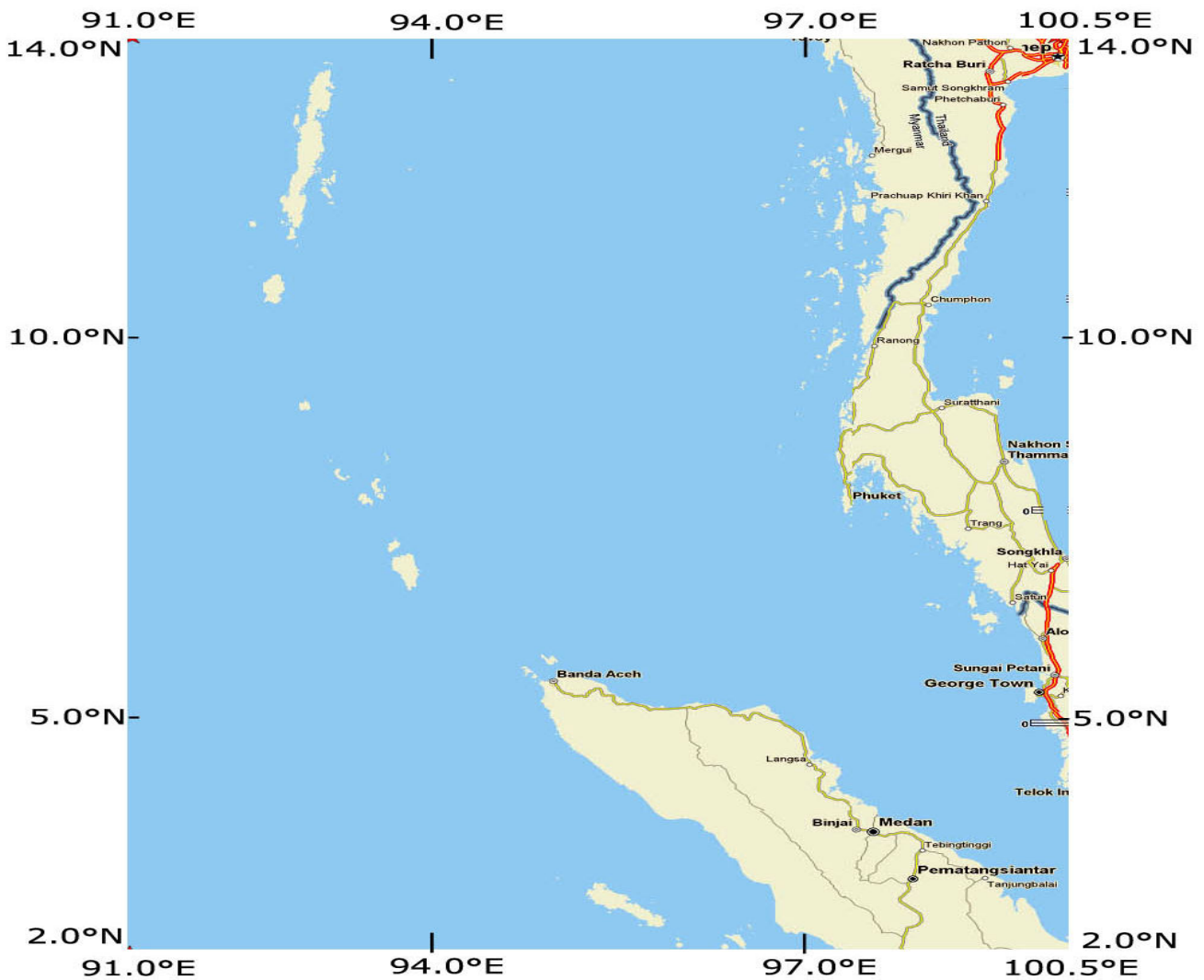

Fig. 1 Outer model domain including west coast of Thailand, Peninsular Malaysia and west of North Sumatra covering the source zone

World Academy of Science, Engineering and Technology
International Journal of Geological and Environmental Engineering
Vol:9, No:8, 2015

Fig. 2 Inner model domain covering Phuket Island in Southern Thailand
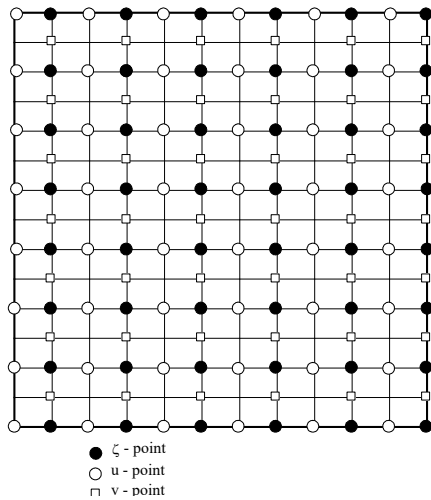

- ● ζ - point
- ○ u - point
- □ v - point

Fig. 3 Staggered grid system that is used in the numerical scheme

II. NUMERICAL MODEL

A. Depth Averaged Shallow Water Equations

To study tsunami events due to sea floor deformation (uplift and subsidence), the equations of continuity and motion are formulated in Cartesian coordinates and the established depth averaged equations of continuity and momentum are

$$\frac{\partial \zeta}{\partial t} - \frac{\partial \eta}{\partial t} + \frac{\partial}{\partial x}[D u] + \frac{\partial}{\partial y}[D v] = 0 \tag{1}$$

$$\frac{\partial u}{\partial t} + u \frac{\partial u}{\partial x} + v \frac{\partial u}{\partial y} - f v = -g \frac{\partial \zeta}{\partial x} - \frac{F_x}{\rho D} \tag{2}$$

$$\frac{\partial v}{\partial t} + u \frac{\partial v}{\partial x} + v \frac{\partial v}{\partial y} + f u = -g \frac{\partial \zeta}{\partial y} - \frac{F_y}{\rho D} \tag{3}$$

u and v denote the velocities in x and y directions, $m\ s^{-1}$, ς is the sea level, η is the sea bed displacement (Fig. 7), g is the earth gravity acceleration, and $D = h + \varsigma - \eta$ is the total ocean depth, f is the Coriolis parameter and is defined by $f = 2\Omega \sin \phi$, φ is the latitude of a location in the analysis area.

The bottom friction forces are defined by

$$F_x = \rho\, C_f\, u \left(u^2 + v^2 \right)^{1/2}$$
$$F_y = \rho\, C_f\, v \left(u^2 + v^2 \right)^{1/2} \tag{4}$$

where, C_f is the coefficient of friction and ρ is the water density, $kg\ m^{-3}$.

B. Model Data Set up

The boundaries of our prototypes are almost never well suited to rectangular geometry unless we use a fine grid. Care must be taken that boundary grid representations in such systems properly approximate the physical boundary. If we want to maintain our structured grid because of its computational advantages, there are two solutions to this problem which are used in practical modeling, the first is to

World Academy of Science, Engineering and Technology
International Journal of Geological and Environmental Engineering
Vol:9, No:8, 2015

use a transformation into a more suitable boundary-fitted curvilinear grid and the second is to use nested grids, in which some regions of the model overlaid with a finer resolution grid. A boundary fitted curvilinear coordinate system is constructed so that the boundaries of the prototype and the computational grid fit together accurately and the grid-lines from smooth defined curves, usually arranged so that they intersect nearly orthogonally.

The outer physical domain of BFNG model with grid size 4km covers the whole model domain including the epicenter of the Indonesian tsunami of 2004.

The time step Δt of the numerical scheme is taken as 10 seconds to ensure the stability of the numerical simulation. Following [12], the value of C_f is taken as 0.0033 throughout the model area. Admiralty bathymetric charts were used to obtain data for ocean depth of the model area.

To solve the model equations we use a conditionally stable semi-implicit finite difference scheme with a staggered grid (Fig. 3). In the numerical scheme the coastal and island boundaries are approximated by continuous segments either along the nearest y-directed odd gridline or along the nearest x-directed even grid line. Thus each boundary is represented by such a stair step that, at each segment there exist only normal component of velocity and this will guarantee the normal vanishing of normal velocity at each boundary. Similar to [8] the origin of the Cartesian coordinate system is taken to be O (3.125° E, 101.5° N), the x-axis is directed towards west at an angle 15° with the latitude line through O and the y-axis is directed towards north inclined at an angle 15° with the longitude line through O.
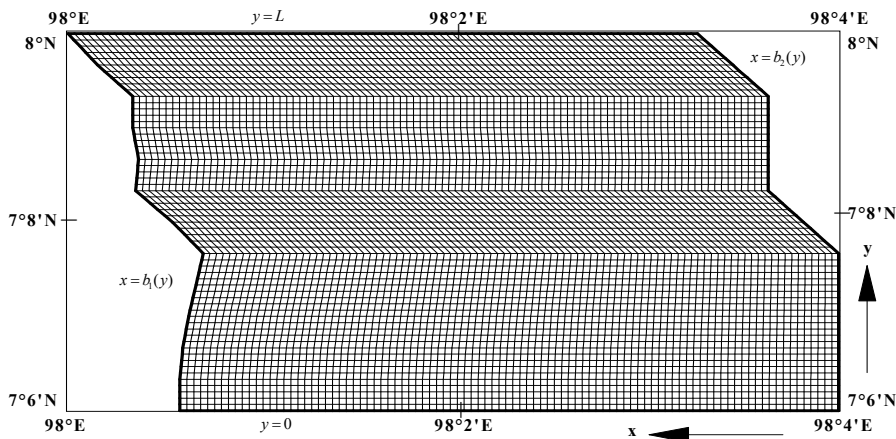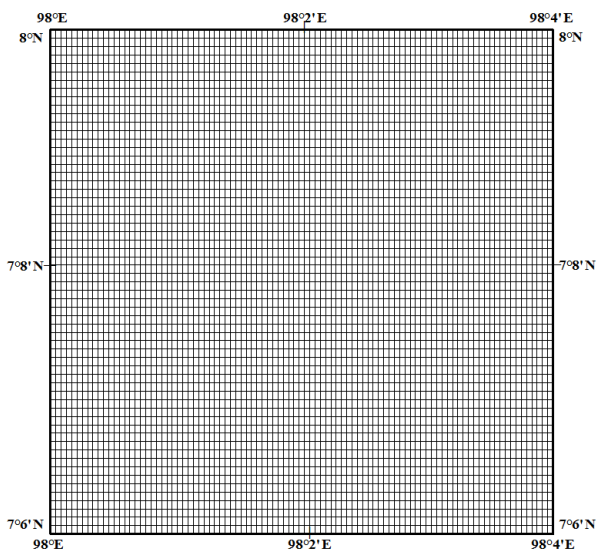

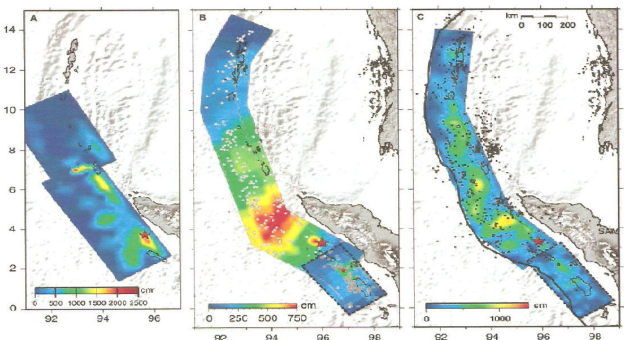Fig. 4 Inner physical domain

Fig. 5 Inner computational domain

Fig. 6 Finite source slip models for the 2004 Sumatra-Andaman Earthquake [2]

C. Boundary Fitted Curvilinear Grid and Coordinate Transformation for Outer and Inner Scheme

Similar to [8] the coastal boundary on the east of the outer physical domain is presented by the function $x = b_1(y)$ while the western open sea boundary of the outer physical domain is defined by the function $x = b_2(y)$. The open ocean boundaries (south and north) are set to be at $y = 0$ and $y = L$ respectively.

World Academy of Science, Engineering and Technology
International Journal of Geological and Environmental Engineering
Vol:9, No:8, 2015

Similar to the outer model the eastern coastal boundary of the inner model (Fig. 4) is represented by $x = b_1(y)$ which is a part of the eastern coastal boundary of the outer model and situated at the same computational grid line. The western open sea boundary of the inner model is represented by $x = b_2(y)$ which is identical with a particular grid line of the outer model parallel to the y-axis. The open ocean boundaries (south and north) are located at two particular grid lines of the outer model parallel to x-axis. The curvilinear grid lines parallel to x and y-axes in the inner model are generated by the two generalized functions same as the outer model. Similar coordinate transformation of [6] is used in treating the curvilinear boundary configuration to rectangular one. The physical and transformed domains are presented in Figs. 4 and 5.

D. Boundary Conditions of Outer and Inner Models

Similar to Karim at al. [8] the radiation boundary conditions for the north, south and west open sea boundaries of outer model are applied in this study. Radiation boundary condition allows the disturbance generated within the model area, to go out through the open boundary. The components of normal velocity are set to zero at the coasts of the main land and islands (i.e. closed boundaries).

The stair-step with coarse mesh (outer model) is nested with fine mesh (inner model) within a parent model so as to increase the accuracy of the ocean depth near the shore of Phuket Island. The outer and inner model domains cover the region between 2° N to14° N latitude; 91° E to 100.5° E longitude and between 7°4′ N to 8°1′ N latitude; 98° E to 98°4′ E longitude. The equal spacing mesh size of the outer domain is set at 4 km and there are 230 x 319 grid points in the computational xy-plane. The equal spacing of the mesh size of the inner domain is set 0.8 km and there are 96 x 61 grid points covering inner domain.

In the nested model, the velocity components along x and y directions and water elevation ζ computed by the outer model in deep ocean are used as the boundary values of the inner models in the offshore region. Computed results obtained from outer model are interpolated and thus use as input into nested model domain as initial conditions. The coupling of the coarser and finer schemes is done according to [6].

III. INITIAL CONDITION (TSUNAMI SOURCE AND ITS IMPLEMENTATION IN OUTER MODEL)

Based on rupture process of the event 26 December 2004 estimated by several authors, a justified tsunami source has been constructed deform and timing of seabed displacement. We consider the source, extended along the fault line between 92–97°E and 2–13.5°N; this zone is a rectangular area having length ~ 1200 km and width ~ 300 km. This rectangular zone has been divided into 42×4 segments as shown in Fig. 8. We designate the segments by S_{ij} where $i = 1, 2, …, 42; j = 1, 2, 3, 4$. Starting from S_{11} at the southwest corner of the rectangular source zone we activate the whole source in 45 time steps (in 450 seconds) in the following way (Table I), Thus, the source has been activated gradually from south to north and from west to east as shown in Fig. 8. Based on the information available in several published papers outlined in the introduction a more realistic source (with maximum uplift of 5 m and maximum subsidence of 4.75 m) of the seabed from west to east is considered in this study. Following the source deformation contours of [12], the magnitude of sea bed deformation in different segments of rupture zone is assigned in our model simulation. The initial sea floor elevations and the velocity components are taken as zero everywhere. Thus the source has been activated gradually from south to north and from west to east as shown in Fig. 8. Based on the information outlined in this section, we consider the source with maximum rise of 5 m and maximum fall of 4.75 m of the seabed from west to east. In our model simulation, the magnitude of sea bed deformation in different segments of rupture zone is taken from the source deformation contours of [12]. The initial sea floor displacement and the velocity components are taken as zero everywhere.

TABLE I
ACTIVATION OF TSUNAMI SOURCE

Time Step	Segment activated							
1	$S_{1,1}$							
2	$S_{2,1}$	$S_{1,2}$						
3	$S_{3,1}$	$S_{2,2}$	$S_{1,3}$					
4	$S_{4,1}$	$S_{3,2}$	$S_{2,3}$	$S_{1,4}$				
…	…	…	…	…	…	…	…	…
k	$S_{k,1}$	$S_{k-1,2}$	$S_{k-2,3}$	$S_{k-3,4}$	$k = 4,5,...$	…	…	$k = 42$
…	…	…	…	…	…	…	…	…
42	$S_{42,1}$	$S_{41,2}$	$S_{40,3}$	$S_{39,4}$				
43	$S_{42,2}$	$S_{41,3}$	$S_{40,4}$					
44	$S_{42,3}$	$S_{41,4}$						
45	$S_{42,4}$							

World Academy of Science, Engineering and Technology
International Journal of Geological and Environmental Engineering
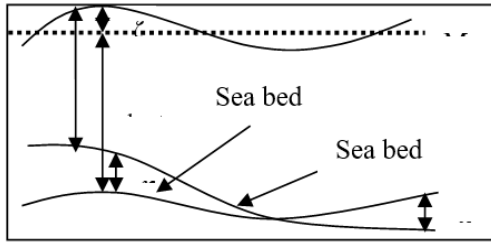Vol:9, No:8, 2015

Fig. 7 Schematic diagram that shows the seafloor deformation (η) and sea surface elevation (ς) from the mean sea level (MSL)
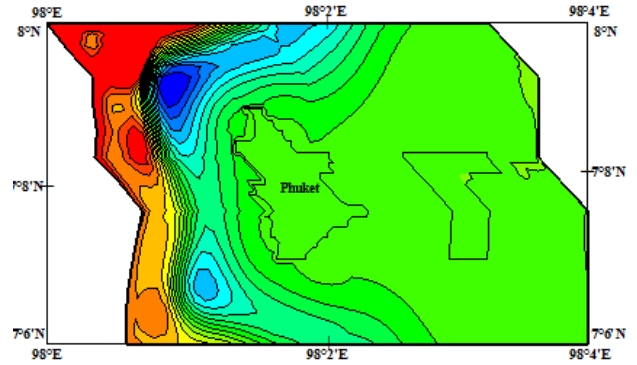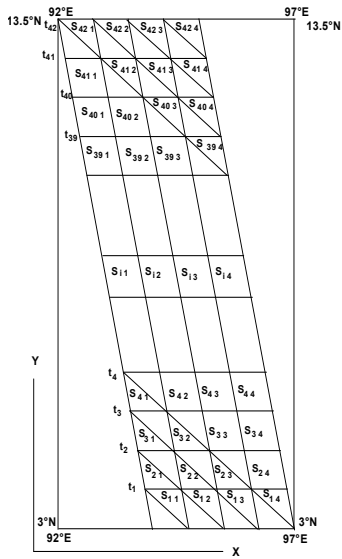

Fig. 8 Tsunami source activated into several segments over a short period of time

Fig. 9 Elevation of Tsunami propagation towards Phuket at 110 minutes
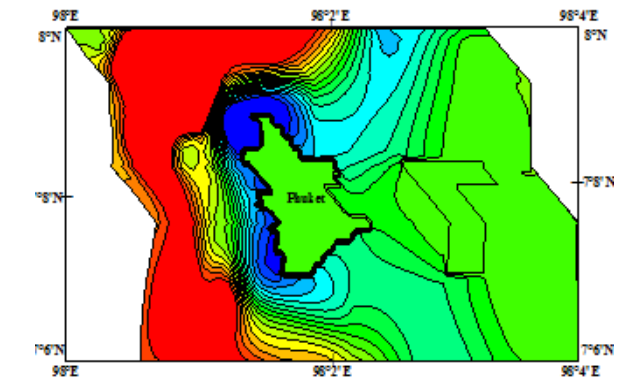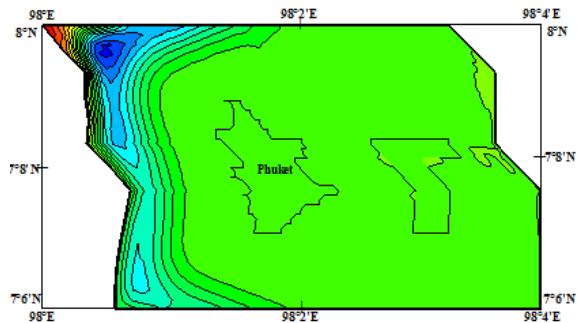

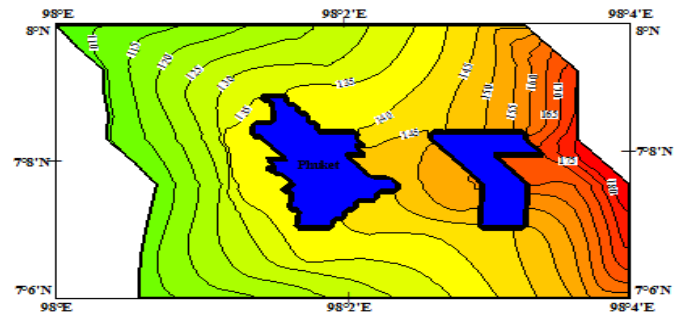Fig. 10 Elevation of Tsunami propagation towards Phuket at 120 minutes

Fig. 11 Elevation of Tsunami propagation towards Phuket at 130 minutes

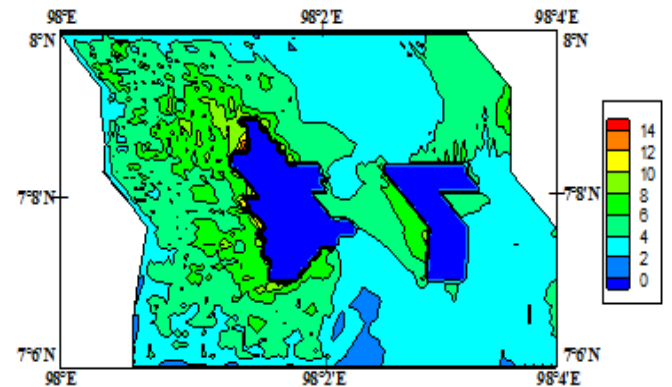Fig. 12 Tsunami arrival time towards Phuket Island

Fig. 13 Maximum water level computed around Phuket Island in Southern Thailand
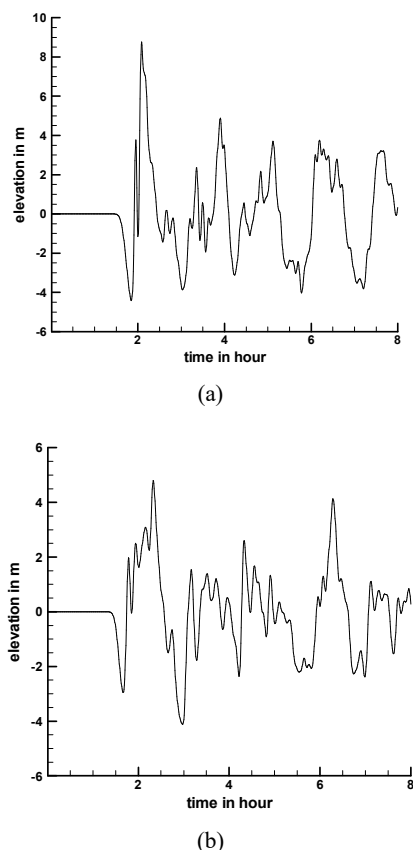
World Academy of Science, Engineering and Technology
International Journal of Geological and Environmental Engineering
Vol:9, No:8, 2015

(a)

(b)

Fig. 14 Time histories of computed elevation at two coastal locations of Phuket Island: (a) North-west (b) East coast

IV. Results and Discussions of BFNG Model

A. Tsunami Propagation towards Phuket

Computed results of propagation from the developed BFNG model Southern Thailand are presented in Figs. 9-11 in the form of contour of sea level enhancement. In these figures the propagation of the tsunami towards Phuket can be seen, where the sea surface disturbance pattern is shown at three different instants of time. The sea surface disturbance is found to be proceeding towards Phuket at 110 min after the generation of the initial tsunami wave at the source (Fig. 9). At 120 min the tsunami has proceeded considerably towards Phuket Island and jammed at western side (Fig. 10) and at 130 min surge flooded the whole Phuket region (Fig. 11).

B. Computed Tsunami Arrival Time and Maximum Water Level along the Coasts

The computed arrival time of tsunami in contour forms at every grid point is presented in Fig. 12. It is observed that the tsunami arrival time to the coastal belts of Phuket (north-west to south-east) is between 130 and 145 min. In general, the travel time increase southward of Phuket. The local bathymetric effects could have played a role. It is reported in USGS that the tsunami reached Phuket Island two hours after the earthquake [13] tsunami travel time in hours for the entire

Indian Ocean)]. Thus the computed result of the BFNG model is close to the observations available in USGS website.

The propagation of tsunami towards the Phuket brings the tsunami amplitude up to 14 m (maximum) at west part of north Phuket. Fig. 13 shows the contour of maximum surge level in the shore of Phuket. The surge amplitude is found to be 3.0 m to 14 m and it is found to be increasing from south to north. The enhancement of sea level is found to be fast when it reaches near the shore. In general the tsunami amplitude has gradually decreased as one goes southward along the shore of Phuket. It is also seen from this figure that the north-west part of Phuket Island are more vulnerable for stronger tsunami. Computed maximum surge levels using the BFNG model are compared with that available in the USGS website [18]. In this website address it is reported that wave height reached 7 to 14 m surrounding Phuket. Satake et al. [18] reported that tsunami heights experienced 5 to 20 m along Southern Thailand coast. Thus, comparison of the BFNG model results with USGS website and [18] are quite satisfactory.

C. Computed Time Series of Water Levels along the Phuket Island

The computed time histories using the BFNG model of sea surface fluctuations at two coastal locations of Phuket Island are stored at an interval of 30 seconds and presented in Fig. 14. At the north-west coast of Phuket, the maximum sea surface level is 8.2 m (2nd crest) and the minimum is – 4.4 m. It is seen that at approximately 1.8 hours after generation of tsunami, instead of water level rise it goes down and reaches up to a level of – 4.4 m. Then the sea level reaches up to 3.6 m (1st crest) at approximately 2 hrs before going down again (Fig. 14 (a)). The sea level begins with a depression of -3.2 m and the maximum sea level reaches up to 4.4 m at the east coast at approximately 2.2 hours after the generation at source (Fig. 14 (b)). In this location also first crest shows low amplitude. The witness and the simulated results in [14] confirm the same behavior that the first wave appears with lower amplitude. In both locations it is observed that the oscillation continues for several hours. Tsuji et al. [19] reported that at first sea level goes down with duration within 45 to 60 min, followed by the rising-up. The eyewitnesses also reported the same feature along the Andaman Sea [19]. Although the computed results we have obtained using the BFNG model for tsunami propagation with reference to arrival time, maximum surge and the time series of sea surface elevation are qualitatively similar to the computed results of our previous studies on Phuket [10]. The results of the BFNG model we have developed show slightly better agreement with available data.

V. Conclusion

The impact of Indonesian tsunami of 2004 along Southern Thailand is studied using the BFNG model. We studied the characteristics of this tsunami, with particular reference to the travel times, maximum wave amplitude and time histories of sea level in coastal locations. Comparisons between the results

World Academy of Science, Engineering and Technology
International Journal of Geological and Environmental Engineering
Vol:9, No:8, 2015

of this study and the available data indicate that BFNG model is a powerful tool for simulating tsunami along a coastal belt, which is curvilinear in nature and bathymetry changes abruptly near the shore. This model can make the grids fit the boundaries and can facilitate the handling of boundary conditions for outer and inner models successfully.

REFERENCES

[1] Abbott, M.B., Damsgaard, A., and Rodenhuis, G.S., "System 21, 'Jupiter' A design system for two-dimensional nearly-horizontal flows", J. of Hydraulic Research, 11(1), 1 -28, 1973.

[2] Ammon, J.C., Ji, C., Thio, H., Robinson, D., Ni, S., Hjorleifsdottir, V., Kanamori, H., Lay, T., Das, S., Helmberger, D., Ichionose, G., Polet, J., and Wald, D., "Rupture Process of the 2004 Sumatra-Andaman Earthquake" Science 308, 1133-1139, 2005.

[3] Falconer, R.A., "Numerical modeling of tidal circulation in harbours", J. Waterway, Port, Coastal and Ocean Div., Proc. ASCE, 106, WW1, 31 – 48, 1980.

[4] Iguchi, T., "A mathematical analysis of tsunami generation in shallow water due to sea bed deformation", Proceedings of the Royal Society of Edinburgh, 141A, 551-608, 2011.

[5] Jones, J. E., and Davis, A. M., "Storm Surge computations for the Irish Sea using a three dimensional numerical model including wave-current interaction", Continental Shelf Research, 18, 201-251, 1998.

[6] Johns, B., Rao, A. D., Dube, S. K., and Sinha, P. C., " Numerical modelling of tide-surge interaction in the Bay of Bengal", Phil. Trans. Roy. Soc. London A 313, 507 – 535, 1985.

[7] Karim, M. F., Roy, G. D., Ismail, A. I. M., and Meah, M. A., " A linear Cartesian coordinate shallow water model for tsunami computation along the west coast of Thailand and Malaysia" Int. J. of Ecology & Development" 4(S06): 1 – 14, 2006.

[8] Karim, M. F., Roy, G. D., Ismail, A. I. M., and Meah, M. A., " A shallow water model for computing tsunami along the west coast of Peninsular Malaysia and Thailand using boundary-fitted curvilinear grids" Journal of Science of Tsunami Hazards, 26 (1), 21 – 41, 2007a.

[9] Karim, M. F., Roy, G. D., and Ismail, A. I. M., "An Investigation on the Effect of Different Orientation of a Tsunami Source along the Coastal Belt of Penang Island: A Case Study of the Indonesian Tsunami 2004" Far East J. of Ocean Research, 1 (1), 2007, 33-47, 2007b.

[10] Karim, M. F., Roy, G. D., Ismail, A. I. M.; and Meah, M.A., "Numerical Simulation of Indonesian Tsunami 2004 along Southern Thailand: A Nested Grid Model", International Journal of Mathematical, Physical and Engineering Sciences, volume 3 (1),8-14, 2009a.

[11] Karim, M. F., Ismail, A. I. M.; and Meah, M.A., "Numerical Simulation of Indonesian Tsunami 2004 at Penang Island in Peninsular Malaysia using a Nested Grid Model, International Journal of Mathematical Models and Methods in Applied Sciences, Issue 1, volume 3, 1-8, 2009b".

[12] Kowalik, Z., Knight, W., and Whitmore, P. M., "Numerical Modeling of the Global Tsunami: Indonesian Tsunami of 26 December 2004" Journal of Sc. Tsunami Hazards. 23(1), 40 – 56, 2005.

[13] Matsutomi, H., Hiraishi, T., Takahashi, T., Matsuyama, F., Harada, K., and Nakusakul, S., "Supartid, S., Kanbua, W., Siwabowon, C., Phetdee, S., Jachoowong, W., and Srivichai, M., "The December 26, 2004 Sumatra Earthquake Tsunami, Tsunami Field Survey around Phuket, Thailand", http://www.drs.dpri.kyoto-u.ac.jp/sumatra/thailand/phuket_survey_e.html, 2004, 2005.

[14] Murty, T. S., Nirupama, N., Nistor, I., and Hamdi, S., " Far-field characteristics of the tsunami of 26 December 2004", ISET Journal of Earthquake Technology, Technical Note, vol. 42, No. 4, 213-217, 2005.

[15] Okada, Y.," Surface Deformation due to Shear and Tensile Faults in a Half Space" Bull, Seism. Soc. Am., 75, 1135 – 1154, 1985.

[16] Roy, G. D., Karim, M. F., and Ismail, A. M., "A Non-Linear Polar Coordinate Shallow Water Model for Tsunami Computation along North Sumatra and Penang Island" Continental Shelf Research, 27, 245–257, 2007.

[17] Roy, G. D., Karim, M. F., and Ismail, A. M., " Numerical Computation of Some Aspects of 26 December 2004 Tsunami along the West Coast of Thailand and Peninsular Malaysia Using a Cartesian Coordinate Shallow Water Model. Far East J. of Applied Mathematics, 25(1), 57-71, 2006".

[18] Satake, K., Okamura, Y., Shishikura, M.,and Fujima, K., "The December 26, 2004 Sumatra Earthquake Tsunami, Tsunami Field Survey around Phuket, Thailand", http://www.drs.dpri.kyoto-u.ac.jp/sumatra/thailand/phuket_survey_e.html,20005b, 2005.

[19] Tsuji, Y., Namegaya, Y., Matsumoto, H., Iwasaki, S., Kanbua, W., Sriwichai, M., and Meesuk, V., "The 2004 Indian tsunami in Thailand: Surveyed run-up heights and tide gauge records" Earth Planets Space, 58, 223-232, 2006.